PCCP

Point defects and related properties of highly co-doped bixbyite In_2O_3†

T. O. Mason,[a] G. B. González,[a] J.-H. Hwang[b] and D. R. Kammler[c]

[a] *Northwestern University, Materials Science and Engineering, 3037 Cook Hall, Evanston, IL, USA 60208. E-mail: t-mason@northwestern.edu; Fax: +1 847 491 7820; Tel: +1 847 491 3198*

[b] *Hongik University, Materials Science and Engineering, 72-1 Songsu-Dong, Mapo-Gu, Seoul 121-791, Korea. E-mail: jhwang@wow.hongik.ac.kr; Fax: +82 2 333 0127; Tel: +82 2 320 3069*

[c] *Sandia National Laboratory, MS 1077, P.O. Box 5800, Albuquerque NM 87185-1077. E-mail: drkamml@sandia.gov; Fax: +1 505 844 7833; Tel: +1 505 845 0297*

Received 6th January 2003, Accepted 22nd April 2003
First published as an Advance Article on the web 6th May 2003

The method of co-doping has been employed to achieve and study the influence of high defect populations in bixbyite In_2O_3. Substantial metastable Sn-doping levels can be achieved in nanocrystalline In_2O_3 with associated co-doping by oxygen interstitials. The resulting electrical properties, diffraction data (X-ray and neutron), and EXAFS studies support the presence of 2 : 1 Sn-oxygen interstitial point defect clusters. Upon reduction, some of these clusters can be reduced to liberate donors and generate charge carriers. Extensive Cd/Sn co-substitution for indium in In_2O_3 has been achieved in equilibrium solid solutions. This self-compensated (isovalent) and relatively size-matched substitution reveals a tendency for off-stoichiometry in favor of donors, resulting in "self-doped" behavior irrespective of oxygen partial pressure. Ramifications of bixbyite defect structure for transparent electrode applications are discussed.

Introduction

Next to tin oxide, indium oxide is the most widely used transparent conductor, especially when donor-doped with tin, so-called indium–tin oxide or ITO.[1] Transparent conductors are used as coatings in energy-efficient windows and as transparent electrodes in photovoltaic cells, flat panel displays, and a variety of opto-electronic devices (*e.g.*, light-emitting diodes). Optimization of TCO (transparent conducting oxide) properties depends upon understanding and controlling the defect structure, which in turn controls carrier content and influences carrier mobility *via* attendant scattering mechanisms.

In_2O_3 crystallizes in the cubic bixbyite structure (space group number 206, $Ia\bar{3}$, $a = 10.117$ Å) with 80 atoms or 16 formula units per unit cell.[2] The structure can be derived from a $2 \times 2 \times 2$ super cell of the fluorite structure by removing $\frac{1}{4}$ of the oxygens to create structural vacancies. Since these positions are available interstitial sites in the bixbyite structure, it is not surprising to find that oxygen interstitials can be formed in co-doped situations (see below). All 16 interstitial sites are symmetry-equivalent, as are the 48 lattice oxygen sites. Two types of indium sites exist in the structure, referred to as b- and d-sites in Wyckoff notation, of which there are eight and 24 per unit cell, respectively. Both b- and d-sites are six-fold coordinated by oxygen in a distorted octahedral geometry, of which the b-site coordination is more regular. All oxygen sites, including interstitial positions, are coordinated by four indium sites, one b-site and three d-sites.

The defect structure of pure and doped In_2O_3 has been well studied over the past 30 years, with significant contributions and/or reviews by several groups.[3–7] In particular, the model of Frank and Köstlin[4] invoking neutral 2 : 1 $(2Sn_{In}^{\bullet}O_i'')^{\times}$ associates, some of which are ionizable and others are non-ionizable (see below) is widely accepted for describing the point defect structure of ITO. Our combined X-ray/neutron diffraction Rietveld analyses of ITO essentially confirmed the Frank and Köstlin model of Sn/O co-doping (local ionic compensation).[7] Recent theoretical[8,9] studies investigated ITO clusters over a range of Sn/O ratios, and suggested that the actual defect structure may be more complicated than originally thought, especially at high Sn levels. Finally, recent work in the Cd–In–Sn–O[10] and Zn–In–Sn–O[11] phase diagrams has revealed the existence of extended co-solubility ranges in $In_{2-2x}Cd_xSn_xO_3$ (out to $x = 0.34$) and $In_{2-2x}Zn_xSn_xO_3$ (out to $x = 0.4$). The present work was devoted to the study of bixbyite defect structure at large co-doping concentrations, both in ITO (Sn/O co-doped samples) and in ternary compositions (Sn/Cd co-doped samples).

As reviewed by Korotkov *et al.*,[12] the subject of co-doping is of considerable academic and technological interest.[13–16] For example, the technique has been utilized to enhance the carrier content in p-type wide bandgap III–V semiconductors. Potential factors in this enhancement are improved solubilities, lowering of ionization energies, and the formation of defect complexes. Although attempts to produce p-type co-doped In_2O_3 have been unsuccessful (see below), we believe ITO to be the quintessential n-type co-doped material.

It was desirable in the present work to achieve as high co-doping levels as possible. This was expected to increase the level of defect pairs and/or complexes in order to better study their influence on structural and physical properties.

† Presented at the 78th International Bunsen Discussion Meeting on "Complex Oxides: Defect Chemistry, Transport and Chemical Reaction", Vaals, The Netherlands, October 6–9, 2002.

DOI: 10.1039/b300171g

Overdoping also served to enhance tin and oxygen interstitial populations (in ITO) for more reliable Rietveld analysis of X-ray and neutron diffraction data. High levels of Cd/Sn co-doping can be readily achieved in equilibrium solid solutions, as mentioned previously.[10] But the equilibrium Sn solubility limit in In_2O_3 is quite low, only 0.5 cation % at 1000 °C rising to 3.5 cation % at 1400 °C.[17] This compares to Zr solubility limits in In_2O_3 of 0.4 cation % at 1400 °C and 1.4 cation % at 1700 °C.[5] However, Sasaki *et al.*[5] showed that fine scale mixing during processing (*e.g.*, by co-precipitation and sintering) could produce much higher "metastable" solubilities of ZrO_2 in In_2O_3—up to 8 ± 2 cation % at 1500 °C and 19 ± 2 cation % at 1000 °C. The kinetics of segregation of the metastable excess ZrO_2 was very slow, *e.g.*, 40 h at 1200 °C and 250 h at 1000 °C. Comparable kinetics were found in the present work for nanocrystalline ITO (see below).

The propensity of the bixbyite structure for metastable overdoping allows for high levels of co-doping to be achieved, thereby facilitating the structural and physical studies of the present work. It should be mentioned that metastable overdoping also accounts for the high Sn-levels that can be achieved in ITO thin films (often 10 or 20 cation % or greater), and possibly for the highly disparate reports of extended Sn-solubility in bulk In_2O_3 made by various processing routes.[18–20] (It should be mentioned that due to peak overlap with bixbyite, minor amounts of the secondary $In_4Sn_3O_{12}$ phase are often overlooked in X-ray diffraction patterns.)

Experimental

Nanocrystalline ITO with 8.7 cation % Sn (by chemical analysis) was obtained from Nanophase Technologies (Romeoville, IL). These powders were produced by physical vapor synthesis and subsequent oxidation. This process achieves the atomic scale mixing necessary to form the extended (albeit metastable) bixbyite solid solution. These powders were found to be phase-pure bixbyite by X-ray diffraction. The Sn content was much larger than the sum of all other aliovalent species (<.1 cation %). Pellets approximately 13 mm in diameter and 2 mm thick were pressed at 125 MPa and cold-pressed isostatically at 280 MPa. They were then sintered lightly at 700 °C for 1 h to approximately 50% theoretical density, with a grain size of 30–40 nm (by SEM). One such pellet was cut by diamond saw into rectangular bars, with dimensions $2 \times 3 \times 8$ mm, for conductivity measurements—both at room temperature and at higher temperatures to study the kinetics of Sn segregation. Some pellets were subjected to a 6 h reduction anneal at 500 °C in forming gas (4% H_2/96% N_2). For purpose of comparison, pellets of undoped indium oxide were pressed from high purity powder, 99.99% In_2O_3 (Aldrich Chemical Co., Milwaukee, WI), sintered at 1350 °C, and air-quenched. Some of these pellets were subsequently reduced at $p_{O_2} = 10^{-14}$ atm in flowing CO/CO_2 at 800 °C for 65 h and quenched to room temperature.

High temperature four-point electrical conductivity measurements were made on the nano-ITO bars at 500 °C under pre-mixed Ar/O_2 gases (1 atm total pressure), over a partial pressure range from 10^{-6} to 1, as confirmed by a down-stream zirconia oxygen sensor. Measurements were taken after stable (equilibrium) values were obtained, typically less than 4 h. A computer-controlled current source (model 224), scanner (model 205) and digital multimeter (model 196) were used for conductivity measurements (Keithley Instruments, Cleveland, OH). Platinum foil (current leads) and wire loop contacts (voltage leads) were attached to the sample and a current reversal technique was employed to correct voltages for thermal emf. Other conductivity measurements were made at room temperature on pellets quenched from higher temperatures (900–1100 °C) to follow the kinetics of Sn segregation (see below).

Time-of-flight (TOF) neutron powder diffraction data were collected on all quenched samples using the Special Environment Powder Diffractometer (SEPD) at the Intense Pulsed Neutron Source (IPNS) located at Argonne National Laboratory (ANL).[21] An incident In_2O_3 spectrum was collected and used to normalize all the diffraction patterns in order to correct for the high absorption of indium in the samples.

High-resolution X-ray powder diffraction data were collected on the nano-ITO samples at the Bending Magnet C of DND-CAT (DuPont-Northwestern-Dow Collaborative Access Team) located at the Advanced Photon Source (APS) of ANL, using a two-circle diffractometer equipped with a Ge (220) crystal analyzer and vertical Soller slits. The powder samples were loaded into glass capillary tubes and run in transmission mode. Diffraction patterns were collected at the In K absorption edge (27 940 eV) and 100 eV below (27 840 eV) to maximize the contrast between the In and Sn cations. The experimental anomalous f' and f'' scattering correction terms at the two energies were obtained by analyzing measured extended X-ray absorption fine structure (EXAFS) scans of the samples with the program Chooch.[22] For each ITO sample, the two X-ray patterns combined with the TOF neutron diffraction data were refined with the Rietveld method[23] using the FullProf program.[24]

EXAFS experiments were conducted at the APS Bending Magnet D station of DND-CAT at ANL. EXAFS spectra of In_2O_3 (oxidized and reduced), SnO_2, and nano-ITO (oxidized and reduced) samples were collected at room temperature in transmission mode at the In (27 940) and Sn (29 200) K absorption edges using a Si (111) monochromator crystal. In_2O_3 and SnO_2 were used as experimental standards for ITO at the In and Sn edges, respectively. The incident ionization chamber was filled with a mixture of Ar and N_2 gases, while the transmitted intensity was measured with an ionization chamber filled with only Ar gas. Various layers of clear adhesive tape covered with powder sample were put together to obtain an edge jump of $\Delta\mu x = 1$ at the In edge and $0.1 < \Delta\mu x < 0.2$ at the Sn edge. Here μ is the linear absorption coefficient and x is the thickness of the specimen. The EXAFS spectra were analyzed using the program WinXAS.[25]

Cd/Sn co-doped In_2O_3 specimens were prepared from high purity (>99.99%) CdO, In_2O_3, and SnO_2 powders (Aldrich Chemical Co., Milwaukee, WI). The component powders were ground and mixed under acetone with an agate mortar and pestle and pressed at 150 MPa in a 6.4 mm diameter die. Pellets were loaded into a cylindrical alumina crucible and buried in a sacrificial bed of their constituent powders to limit volatilization and contamination from the crucible. A tightly fitting alumina tube sealed at one end was then lowered around the crucible as an additional evaporation barrier. Pellets were calcined for 20–24 h at 1000 °C, quenched in air, reground and re-pelletized, and fired at 1175 °C until reaction was complete. This also served to densify pellets for room temperature electrical measurements.

The DC conductivities of quenched pellets (nano-ITO and Cd/Sn-doped In_2O_3) were measured at room temperature in an osmium-tipped (radii = 0.254 mm) four-point probe apparatus (Cascade Microtech, Beaverton, OR) interfaced with a constant current source (Model 224) and digital voltmeter (model 195A) from Keithley Instruments (Cleveland, OH). The results were corrected for finite sample diameter and thickness.[26]

Discussion and experimental results

Point defect background

Before presenting and interpreting the experimental results, a brief description of the defect structure of pure, lightly doped, and heavily doped In_2O_3 is in order. There is strong consensus in the literature that the prevailing point defects in undoped

In_2O_3 are oxygen vacancies and electrons, which form according to:

$$O_O^{\times} \rightleftharpoons \tfrac{1}{2}\ O_2(g) + V_O^{\cdot\cdot} + 2e' \quad (1)$$

(in Kröger–Vink notation). The associated $-1/6$ slope in log(conductivity) *vs.* $\log(p_{O_2})$ was clearly obtained under equilibrium conditions by de Wit,[3] Maruyama *et al.*,[27] and Sasaki *et al.*[5]

Light doping is either ionically compensated (*e.g.*, $2[V_O^{\cdot\cdot}] = [Mg'_{In}]$, as in ref. 3) for acceptors or electronically compensated (*e.g.*, $n = [Zr_{In}^{\cdot}]$ as in ref. 26) for donors, consistent with the majority species above. In the latter case, the electron population was fixed by the Zr-donor doping, and the oxygen diffusion coefficient exhibited the $-1/2\ \log(D)$ *vs.* $\log(p_{O_2})$ dependence predicted by eqn. (1) for vacancy diffusion when n is constant. Under oxidizing conditions, however, a $+1/2\ \log(D)$ *vs.* $\log(p_{O_2})$ dependence was observed. This was interpreted as arising from oxygen interstitials, whose p_{O_2} dependence should be inverse that of the oxygen vacancies according to the anion Frenkel reaction:

$$O_O^{\times} \rightleftharpoons O_i'' + V_O^{\cdot\cdot};\ K_F = [O_i''][V_O^{\cdot\cdot}] \quad (2)$$

It should be stressed that these interstitials must be minority species, since they do not influence the prevailing electroneutrality condition ($n = [Zr_{In}^{\cdot}]$).

With acceptor doping, ionic compensation (*e.g.*, $2[V_O^{\cdot\cdot}] = [Mg'_{In}]$, as in ref. 3) is strongly favored over electronic compensation (*e.g.*, $p = [Mg'_{In}]$). Substituting this into the mass action relationship for eqn. (1):

$$K_1 {p_{O_2}}^{-\frac{1}{2}} = [V_O^{\cdot\cdot}]n^2 = \{[Mg'_{In}]/2\}n^2 \quad (3)$$

it follows that the electron population should vary with the acceptor concentration to the $-\frac{1}{2}$ power. This has been observed experimentally in Mg-doped In_2O_3.[3] It should be stressed that there should be a concomitant increase of electron holes with acceptor doping according to:

$$\text{null} \rightleftharpoons e' + h^{\bullet},\ K_i = np \quad (4)$$

i.e., $p \propto [Mg'_{In}]^{\frac{1}{2}}$, however this cannot be confirmed. There is no evidence of p-type behavior having ever having been obtained in acceptor-doped In_2O_3.

As pointed out above, high levels of donor doping are possible, at least metastably, in bixbyite. Frank and Köstlin[4] are credited for postulating the existence of neutral 2 : 1 associates, *i.e.*, $(2Sn_{In}^{\cdot}O_i'')^{\times}$. Their evidence included a ${p_{O_2}}^{-1/8}$ dependence of the electron population (in the high p_{O_2} regime) along with a $[Sn_{tot}]^{1/4}$ doping dependence. Both derive from the following point defect reaction:

$$(2Sn_{In}^{\cdot}O_i'')^{\times} \rightleftharpoons \tfrac{1}{2}\ O_2(g) + 2Sn_{In}^{\cdot} + 2e' \quad (5)$$

under the condition that $[(2Sn_{In}^{\cdot}O_i'')^{\times}] \gg [Sn_{In}^{\cdot}]$, which occurs at intermediate doping levels under oxidizing conditions. Although the Frank and Köstlin work was on overdoped ITO thin films, Sasaki *et al.*[5] confirmed the ${p_{O_2}}^{-1/8}$ behavior for conductivity in bulk Zr-doped In_2O_3. Frank and Köstlin also observed an exhaustion regime at intermediate values of p_{O_2}, where the electron concentration became p_{O_2}-independent. This follows from the reaction in eqn. (5) when $[Sn_{In}^{\cdot}] \gg [(2Sn_{In}^{\cdot}O_i'')^{\times}]$, *i.e.*, the reaction goes essentially to completion. Similarly, Sasaki *et al.*[5] and Hwang *et al.*[6] obtained this exhaustion regime in highly Zr-doped and Sn-doped bulk specimens, respectively.

Based on their finding that the carrier content was significantly smaller than the overall Sn doping level in the exhaustion regime, Frank and Köstlin[4] hypothesized that a fraction of their 2 : 1 associates were non-ionizable. They suggested that associates where the Sn species were first near neighbors to one another and also to an oxygen interstitial would so tightly bind the interstitial that the associate would be non-ionizable, *e.g.*, it could not be reduced as in eqn. (5). The ionizable 2 : 1 associates, on the other hand, involved non-adjacent Sn cations and a less tightly bound oxygen interstitial.

Results from the present work

To test whether or not the high Sn-content of the nano-ITO material was truly metastable against Sn-segregation, presintered pellets (700 °C for 1 h) were held at 1100 °C using the sacrificial bed procedure outlined above, and quenched to room temperature for conductivity measurements and phase analysis by X-ray diffraction. The conductivity increased with time (confirming their initial overdoped state) and the initially phase-pure material began to show an increasing presence of rutile SnO_2 in the X-ray patterns. Both the conductivity and SnO_2 content gradually reached asymptotic values after ~400 h of annealing. Based on the starting Sn-content of the nano-ITO and the ultimate SnO_2 content in the equilibrated specimens, the equilibrium Sn-solubility in ITO at 1100 °C was estimated to be ~1 cation %, in good agreement with Ohya *et al.*,[17] who found the solubility to be 0.5 cation % at 1000 °C and 2.0 cation % at 1300 °C. The Sn-segregation time of 400 h is comparable in magnitude to that found in the Zr-doped In_2O_3 by Sasaki *et al.*[5], 40 h at 1200 °C and 250 h at 1000 °C. Ongoing work indicates that the segregation time grows to > 1000 h at 1000 °C, thereby confirming that nano-ITO is quite stable against Sn-segregation at temperatures less than 700 °C.

The electrical conductivity of nano-ITO in the present work (500 °C) is plotted *vs.* oxygen partial pressure in Fig. 1. Both the characteristic ${p_{O_2}}^{-1/8}$ dependence at high p_{O_2} and the onset of the exhaustion regime at lower p_{O_2} values are observed, in agreement with eqn. (5). This is actually quite surprising, given the high level of co-doping (8.7 cation % Sn and ~5% of oxygen interstitials, on a per cation basis, see below). A slightly shallower slope was obtained for thermopower in the high p_{O_2} regime, which was interpreted in terms of the highly degenerate character of this material in ref. 6.

The results obtained from the combined Rietveld refinements are summarized in Table I. The refined total Sn content of the nano-ITO samples is in excellent agreement with the value obtained by chemical analysis (8.7 cation%). Interstitial oxygen populations are present in both nano-ITO samples and absent for pure In_2O_3 samples, in agreement with our previous observations for bulk-ITO.[28] The values obtained for nano-ITO are quite large (6–10% of the interstitial positions occupied), with relatively small uncertainties in the refined concentrations. The ratio of total Sn to oxygen interstitials (Sn/O_i) was 1.7(1) in the oxidized (as-fired) nano-ITO. This

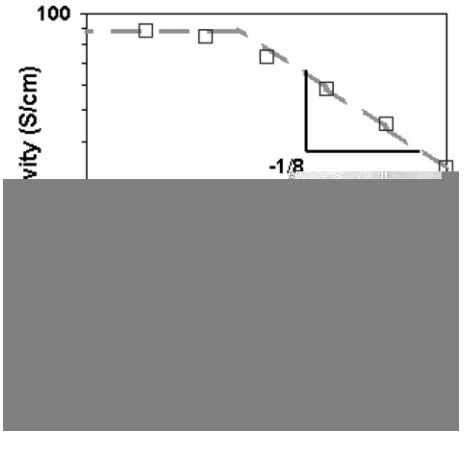

Fig. 1 Conductivity *vs.* p_{O_2} for nano-ITO at 500 °C.

Table 1 Structural results and refinement parameters obtained from combined Rietveld refinement

	In_2O_3 oxidized	In_2O_3 reduced	Nano-ITO oxidized	Nano-ITO reduced
Cation b ($x = y = z = 1/4$)				
B/Å^2	0.45(3)	0.40(3)	0.57(5)	0.40(5)
Sn/[In + Sn]	0	0	0.25(5)	0.15(4)
Cation d ($x, y = 0, z = 1/4$)				
B/Å^2	0.38(2)	0.36(3)	0.31(3)	0.32(2)
x	0.4660(1)	0.4664(1)	0.4687(1)	0.4679(1)
Sn/[In + Sn]	0	0	0.03(1)	0.06(1)
O_s (structural oxygen)				
B/Å^2	0.50(2)	0.50(2)	0.61(3)	0.46(3)
x	0.3904(1)	0.3905(1)	0.3895(2)	0.3900(1)
y	0.1546(1)	0.1546(1)	0.1541(1)	0.1542(1)
z	0.3820(1)	0.3820(1)	0.3818(1)	0.3817(1)
O_i (interstitial oxygen)[a]				
x	0.085[b]	0.085[b]	0.091(1)	0.085(2)
O_i fraction	−0.008(6)	−0.001(6)	0.104(8)	0.057(7)
Total Sn %			8.6	8.7
Sn/O_i			1.7(1)[c]	3.1(3)[c]
a/Å	10.1206(1)	10.1202(1)	10.1288(5)	10.1336(5)
Refinement parameters				
$R_{Bragg\text{-}X\text{-}ray\text{-}below\text{-}In\text{-}edge}$	5.1		2.6	2.2
$R_{Bragg\text{-}X\text{-}ray\text{-}at\text{-}the\text{-}In\text{-}edge}$			6.2	5.0
$R_{Bragg\text{-}neutron}$	2.0	2.3	5.5	4.9
$R_{wp\text{-}below\text{-}In\text{-}edge}$	4.3		8.2	6.7
$R_{wp\text{-}X\text{-}ray\text{-}at\text{-}the\text{-}In\text{-}edge}$			6.1	6.6
$R_{wp\text{-}neutron}$	4.9	4.7	7.2	3.6
χ^2	1.4	1.3	1.7	1.6

[a] $B(O_i)$ was fixed to $B(O_s)$. [b] $x = y = z$ for pure In_2O_3 was fixed to $x = y = z$ for oxidized ITO. [c] Based upon O_i uncertainties only, given the agreement between total Sn contents and the independent chemical analyses (8.7% Sn).

Table 2 EXAFS results

	Coordination number	First nn distance/Å[a]	Residual (%)
In edge			
Oxidized nano-ITO	6.0	2.18	1.3
Reduced nano-ITO	6.0	2.19	3.4
Sn edge			
Oxidized nano-ITO	6.5	2.07	5.0
Reduced nano-ITO	6.3	2.07	3.4

[a] nn means nearest neighbor.

compares with a value of 2.2(3) in oxidized bulk ITO.[28] These values bracket the ideal value of 2.0 corresponding to strictly 2 : 1 $(2Sn_{In}^{\bullet}O_i'')^{\times}$ associates.

Upon reduction in forming gas the Sn/O_i ratio increases to 3.1(3) in nano-ITO. A significantly larger value was obtained for bulk-ITO reduced in CO/CO_2 ($p_{O_2} \sim 10^{-14}$ atm) at 800 °C, Sn/O_i = 6.2(2.2).[28] Both values support the contention that only a portion of the 2 : 1 associates are ionizable; complete ionization would otherwise yield an infinite Sn/O_i ratio, *i.e.*, no remaining oxygen interstitials. It should be noted that, within experimental uncertainty, there is no detectable change in b-site *vs.* d-site tin occupancy with reduction.

There is a noticeable increase in lattice parameter upon reduction of nano-ITO, in agreement with prior work.[4,6,29,30] Frank and Köstlin[4] attributed this to the removal of the compensating (electron-trapping) oxygen interstitials from 2 : 1 clusters, and subsequent repulsion between the two Sn^{4+} ions which cannot be completely compensated by the free electrons.

The Rietveld refinements also suggest a marked preference for Sn occupation of b-sites over d-sites in nano-ITO, in agreement with prior Mössbauer[30] and diffraction studies.[28] Myrasov and Freeman[31] carried out FLMTO electronic structure calculations of In_2O_3 with 1/16 of the In cations replaced by Sn (6.5 cation% Sn). They found a weak (0.05 eV) preference for Sn at the b-site over the d-site but did not consider point defect associates. In contrast, Warschkow *et al.*[8] employed embedded cluster density functional methods to examine the energetics of defect clusters involving Sn in various configurations with oxygen interstitials. They found a negligible difference between the energies of isolated Sn on b-sites *vs.* d-sites, however the tendency to favor b-sites increased with the number of Sn-ions surrounding an oxygen interstitial, in the order 1 : 1 < 2 : 1 < 3 : 1. The b-site preference detected in the present work is therefore consistent with the existence of Sn–O_i associates.

The EXAFS results for nano-ITO in Table 2 also support the existence of Sn–O_i associates. In the In_2O_3 structure, the b site has six oxygens as nearest neighbors at a distance of 2.18 Å, while the d site has six oxygens at an average distance of 2.18 Å (two at 2.13 Å, two at 2.19 Å and two at 2.23 Å). In the SnO_2 structure, Sn has six nearest neighbors at an average distance of 2.04 Å (four nearest neighbors at 2.03 Å and two others at 2.07 Å). While typical errors in coordination numbers obtained from EXAFS refinements are on the order of 10%, errors in distances are about 0.01 Å. Although EXAFS is not accurate enough to detect small changes between the In and Sn coordination numbers, it is quite accurate to detect variations in shell distances. Parent *et al.*[29] found, for a 10% Sn– ITO sample, a splitting in the Sn–O distance and coordination number: five neighbors at 2.027 and 1.6 neighbors at 2.153 (or an average of 6.6 neighbors at an average distance of 2.06 A). Nadaud *et al.*[30] did not observe a splitting but found the coordination number to be 6.1 at a distance of 2.00 for a 6% Sn ITO sample. In the present study splitting was not observed either. In the oxidized and reduced nano-ITO samples indium is found to be coordinated to six atoms at the same In–O distance as in In_2O_3 (2.18 Å). However, at the Sn edge the distances are much shorter (2.07 Å *vs.* 2.18 Å) confirming that oxygens strongly prefer to be near Sn than near In. This preference for oxygen to be closer to Sn than to In is observed in both oxidized and reduced ITO samples.

The calculations of Warshkow *et al.*[8,9] provide important insight concerning the "ionizable" and "non-ionizable" Sn–O_i associates in ITO. Contrary to the suggestion by Frank and Köstlin[4] that non-ionizable clusters involved immediately adjacent Sn cations tightly bound to an oxygen interstitial,[4] they found quite similar interstitial "detachment energies" regardless of the configuration of Sn cations about the oxygen interstitial.[9] What yielded a significant increase in detachment energy was an increase in the number of Sn-ions in a cluster (1 : 1 < 2 : 1 < 3 : 1, *etc.*). Furthermore, they proposed that the linking of two 2 : 1 neutral clusters as in Fig. 2a would yield local environments resembling a tightly bound 3 : 1 cluster (on the left) and a less tightly bound 2 : 1 associate (on the right). Based upon the increased binding energy of a 3 : 1 cluster,[8] they hypothesized that the interstitial on the left would be "non-ionizable" whereas the interstitial on the right would be "ionizable". Reduction would increase the overall Sn/O_i ratio from 2 to 4 (*e.g.*, at intermediate doping levels). However, if both ends of the central 2 : 1 constituent associate are linked to adjacent 2 : 1 associates as in Fig. 2b (*e.g.*, at high doping levels), only the central oxygen interstitial would be "ionizable"; reduction would increase the Sn/O_i ratio from 2 to 3, since it yields two 3 : 1 clusters. It may be entirely fortuitous that the value obtained for reduced nano-ITO, 3.1(3), agrees with a predominance of 3 : 1 clusters. For example, further reduction might shift the Sn/O_i ratio to still larger values. Nevertheless, the results point to an increase in the

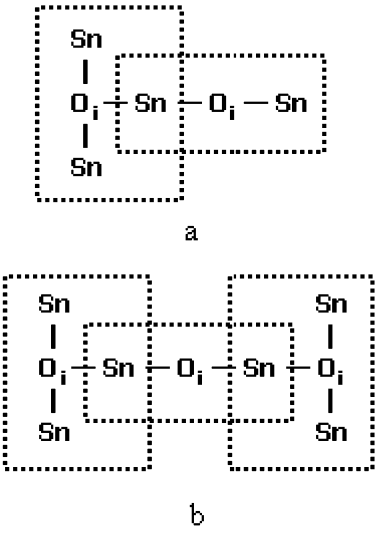

Fig. 2 Clustering of Sn–O_i in ITO (a) environment around the O_i on the left resembles a 3 : 1 cluster, whereas that around the O_i on the right resembles a 2 : 1 cluster, (b) when the O_i in the middle is removed during reduction, two 3 : 1 clusters remain.

amount of "non-ionizable" clusters with doping, *e.g.*, $Sn/O_i = 6.2(2.2)$ in reduced 4.5 cation% Sn-doped bulk ITO[28] *vs.* $Sn/O_i = 3.1(3)$ in reduced 8.7 cation% Sn-doped nano-ITO in the present work.

As mentioned previously, an alternative means of co-doping In_2O_3 is by replacing two In^{3+} cations with one Cd^{2+} and one Sn^{4+}. The replacement reaction (ignoring the difference between b- and d-sites) is:

$$CdO + SnO_2 + 2\ In_{In}^{\times} \rightarrow In_2O_3 + Cd'_{In} + \dot{Sn}_{In} \qquad (6)$$

from which it is clear that this is an isovalent (self-compensated) substitution, *i.e.*, $[Cd'_{In}] = [\dot{Sn}_{In}]$. Fig. 3 shows the Vegard's law behavior of the lattice constant of co-doped bixbyite *vs.* x in $In_{2-2x}Cd_xSn_xO_3$. The extended co-solubility (to $x = 0.34$) is attributable to its isovalent nature and the fact that the average of Cd^{2+} ions (0.95 Å) and Sn^{4+} ions (0.69 Å) in octahedral coordination (0.82 Å) is only slightly larger than that of In^{3+} (0.8 Å).[32] This does not, however, account for the predominant n-type character of all compositions.

To study the effect of excess acceptor *vs.* excess donor doping of co-doped compositions, the following experiments were

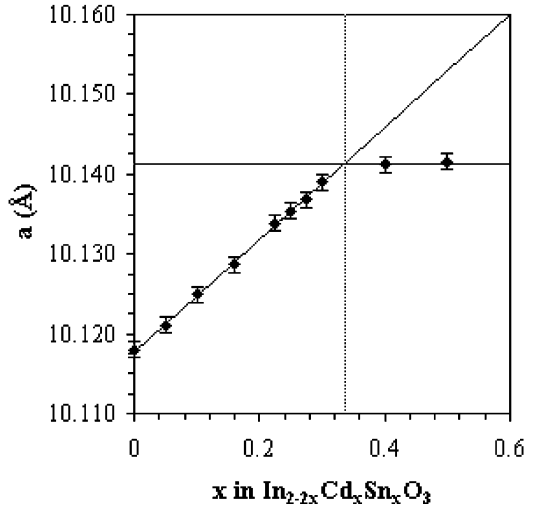

Fig. 3 Lattice parameter as a function of x in $In_{2-2x}Cd_xSn_xO_3$.

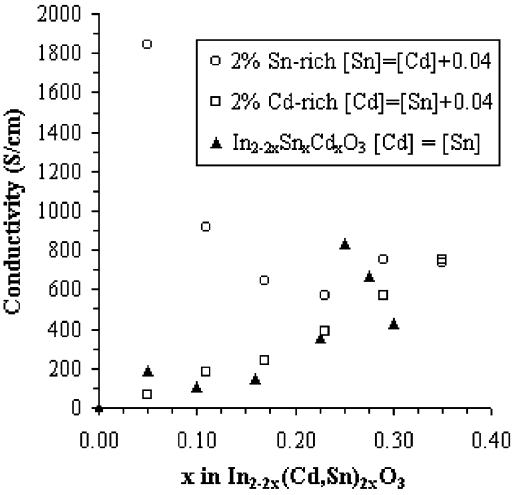

Fig. 4 Conductivity *vs.* x in $In_{2-2x}(Cd,Sn)_{2x}O_3$.

carried out. In addition to nominally cation-stoichiometric $In_{2-2x}Cd_xSn_xO_3$ compositions, intentionally 2% Cd-rich and 2% Sn-rich specimens were prepared at approximately $x =$ 0.05 increments. For example, the 2% Cd-excess material at $x = 0.2$ had the composition, $In_{1.60}Cd_{0.24}Sn_{0.16}O_3$. All excess doped specimens had a minor quantity of second phase by XRD, Cd-doped samples showed $CdIn_2O_4$–Cd_2SnO_4 spinel and Sn-doped samples showed SnO_2, sufficient to saturate the bixbyite at the corresponding solubility limit, but insufficient in the microstructure to significantly alter the electrical properties.

Fig. 4 shows the room temperature electrical conductivity data for all three sets of specimens. Since the relative densities were low (46–60%) the conductivity values were corrected for the influence of porosity using the Bruggeman symmetric medium equation for continuous interconnected porosity (*i.e.*, a 3 : 3 composite).[33] In spite of some scatter, the Cd-excess samples are virtually indistinguishable from the nominally stoichiometric samples. This suggests that Cd/Sn co-doped In_2O_3 cannot tolerate excess acceptors. This is in contrast to our previous work on Zn/Sn co-doped In_2O_3, where an $x = 0.2$ specimen (in $In_{2-2x}Zn_xSn_xO_3$) was shown to accommodate up to 4% excess Zn.[34]

On the other hand, the Sn-excess compositions exhibit significantly higher conductivities than the nominally stoichiometric or Cd-excess samples in Fig. 4. This is consistent with either straight donor-doping ($n = [\dot{Sn}_{In}]$) or a combination of isolated donors and neutral Sn–O_i clusters/associates, as in ITO. There are two interesting features of the conductivity trend, however. After an initial drop of a factor of two (between $x = 0.05$ and $x = 0.10$), the conductivities of the Sn-excess samples become relatively independent of composition (within experimental uncertainty) out to $x = 0.34$. This is in contrast to the Zn/Sn co-doped In_2O_3, where conductivity falls steadily with increasing x in $In_{2-2x}Zn_xSn_xO_3$.[35] One potential implication of the difference between these two systems is that a combination of Zn plus Sn is not as effective as Cd plus Sn in maintaining conductivity when co-substituted for indium. Shannon *et al.*[36] argued that Cd^{2+}, In^{3+}, and/or Sn^{4+} (*not* Zn^{2+}) in octahedral coordination were required for optimal TCO behavior, which was recently substantiated in our review of defect chemistry in the Cd–In–Sn–O system.[7]

The second interesting feature of the conductivity *vs.* composition trends in Fig. 4 is their approximate convergence beyond $x = 0.2$. Sn-excess, stoichiometric, and Cd-excess samples have virtually identical conductivities. This suggests that the phase field width narrows with increasing x in $In_{2-2x}Cd_xSn_xO_3$. Fig. 5 shows the In_2O_3 end of the

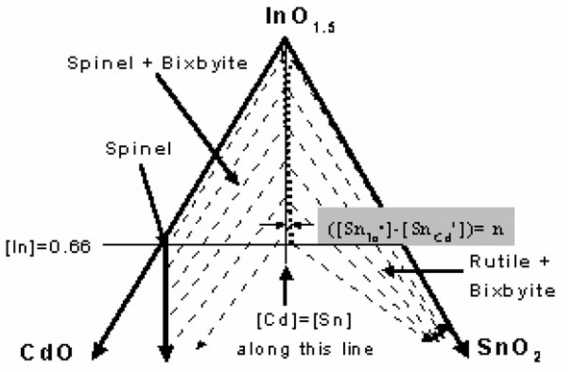

Fig. 5 The bixbyite primary field (after Kammler *et al.*[37]).

Cd–In–Sn–O phase diagram at 1175 °C in air and our proposed phase field behavior for the co-doped solid solution. In separate experiments it was found that whereas pellets of $x \leq 0.10$ were quite sensitive to H_2-reduction (in 4% H_2/96% N_2) at 500 °C, *i.e.*, their conductivities increased significantly during reduction, pellets of $x \geq 0.2$ were relatively insensitive to H_2-reduction. We have interpreted these results as indicative of an inherent cation off-stoichiometry in favor of donors over acceptors, *i.e.*, $[Sn_{In}^{\bullet}] > [Cd_{In}']$.[37] The stability range must shift relative to the ideal stoichiometric line in favor of Sn-excess compositions, as shown in Fig. 5. Tin excess was confirmed by chemical analysis (*via* induction coupled plasma atomic emission spectroscopy) of nominally stoichiometric compositions at higher values of co-substitution.[37]

It is clear that co-doping greatly enhances the solubility of both dopants in the bixbyite structure, especially given the size match with the host and isovalent character of the co-substitution. As mentioned above, we found the equilibrium solubility limit for SnO_2 in In_2O_3 to be 1 cation % at 1100 °C. Similarly, we found the equilibrium solubility limit for CdO in In_2O_3 at 1175 °C to be 1 cation % or less.[10] This is to be compared with 34% cation co-doping in In_2O_3 by CdO and SnO_2 at 1175 °C.

The origin of the inherent donor-to-acceptor excess in Cd/Sn co-doped bixbyite is not as well understood. Warschkow and Ellis[38] have recently found by embedded cluster local density functional methods that Zn-oxygen vacancy associates are energetically favored in Zn-doped In_2O_3. Lightly Zn/Sn co-doped In_2O_3 (analogous to Cd/Sn co-doped In_2O_3[11]) could be a superposition of Zn–V_O associates and Sn–O_i associates. As previously mentioned, Ambrosini *et al.*[34] successfully doped 20% Zn/Sn co-substituted In_2O_3 with up to 4 cation% excess Zn. Isolated Zn^{2+} cations should be acceptors in In_2O_3, but the specimens remained n-type (although with reduced conductivity), therefore supporting the existence of neutral Zn–$V_O^{\bullet\bullet}$ associates. The 2 : 1 A-D-A analogue of the 2 : 1 D-A-D neutral associate in ITO $(2Sn_{In}^{\bullet}O_i'')^{\times}$ would be $(2Zn_{In}'V_O^{\bullet\bullet})^{\times}$, for which there is only this indirect evidence as of the present time. If such species exist and are less favorable energetically than the 2 : 1 $(2Sn_{In}^{\bullet}O_i'')^{\times}$ associates, this may be responsible for shifting the phase field in the direction of Sn-excess compositions.

In Cd/Sn co-doped In_2O_3, however, the evidence does not support the existence of Cd-excess compositions. Furthermore, at higher co-doping levels it would seem reasonable to expect the oxygen interstitials in Sn–O_i associates to cancel with the oxygen vacancies in Cd–V_O associates, leading to Cd–Sn pairs. Embedded cluster LDA calculations show that such pairs are energetically favorable,[38] but cannot to date explain the attendant tendency for donor-excess behavior.

The situation in Cd/Sn co-doped In_2O_3 may be analogous to that in Cd/Sn co-doped $CdIn_2O_4$ spinel. Both exhibit large co-substitution ranges, the later out to $x = 0.75$ in $Cd(In_{2-2x}Cd_xSn_x)_2O_4$, with most of the replacement taking place on octahedrally coordinated sites,[39] as in bixbyite. Zhang and Wei[40] used first-principles total energy calculations on the $x = 1$ end member, Cd_2SnO_4 (stable in thin film form), and accounted for its "self-doping" character (*i.e.*, persistently n-type conductive behavior) on the basis that $Sn_{Cd}^{\bullet}$ donors were far more stable than Cd_{Sn}' acceptors. We have previously argued for an inherent cation off-stoichiometry (donor excess behavior) in the $CdIn_2O_4$–Cd_2SnO_4 spinel solid solution based upon its self-doped character.[7] Like with the co-doped bixbyite phase, intentionally Cd-excess materials are nearly as conductive (and n-type) as Sn-excess materials.

Conclusions and ramifications

The existence of neutral 2 : 1 $(2Sn_{In}^{\bullet}O_i'')^{\times}$ associates in highly Sn-doped (8.7 cation % Sn) indium oxide was confirmed by *in situ* electrical conductivity measurements, plus Rietveld analysis of X-ray and neutron diffraction data and EXAFS experiments on quenched nano-ITO specimens. The preparation method and nanocrystalline material employed allowed for doping levels to be achieved well beyond the equilibrium solubility limit of Sn in bulk In_2O_3. At 500 °C the electrical conductivity exhibited the $p_{O_2}^{-1/8}$ dependence characteristic of the ionization of $(2Sn_{In}^{\bullet}O_i'')^{\times}$ associates. Rietveld analyses of X-ray and neutron diffraction data established that significant populations of oxygen interstitials (up to ~5% on a per cation basis) were present in both oxidized (as-fired) and reduced (forming gas treated) specimens. The Sn/O_i ratio increased from 1.7(1) in oxidized material to 3.1(3) in reduced material. The residual oxygen interstitial concentration of the reduced ITO is consistent with the presence of "non-ionizable" Sn–O_i associates or clusters. The EXAFS results are also consistent with Sn–O_i associates. The Sn nearest neighbor distance of 2.07 Å (both oxidized and reduced samples) is close to that in pure SnO_2 while the In nearest neighbor distance is 2.18 Å as in pure In_2O_3.

Highly Cd/Sn co-doped In_2O_3 was prepared by equilibrium solid state methods 1175 °C in air. It was found that up to 34% of the indium could be successfully replaced *via* co-doping. This is attributable to the approximate size match of (Cd^{2+}/Sn^{4+}) *vs.* $(2In^{3+})$ and the isovalent nature of the substitution. Room temperature electrical conductivity measurements showed a decreasing Sn– *vs.* Cd-excess variability and reduced p_{O_2}-sensitivity as co-doping, *i.e.*, x in $In_{2-2x}Cd_xSn_xO_3$, increased. This was attributed to an inherent off-stoichiometry in favor of donors, *i.e.*, $[Sn_{In}^{\bullet}] > [Cd_{In}']$.

This work suggests that co-doping plays an important role in the development of optimal transparent conducting oxide (TCO) behavior. It is conceivable that Sn–O_i co-doping is responsible, at least in part, for the large metastable Sn-solubility in In_2O_3. The defect associates which are ionizable are largely responsible for carrier generation during the subsequent reduction anneal which is typically carried out on ITO. The same defect associates may also play a role in improving carrier mobility, by replacing long-range Coulomb (ionized impurity scattering) with short-range dipole scattering.

The extensive co-doping of In_2O_3 with Cd^{2+} (or Zn^{2+}) and Sn^{4+} also has important ramifications for TCO development. First, substantial replacement of the much more expensive indium (up to 34–40%) can be accomplished. Second, the TCO properties (electrical and optical) vary continuously with co-substitution, resulting in compositionally-tailorable properties, *e.g.*, band gap and work function. For instance, in as-fired Cd/Sn co-doped In_2O_3 the optical gap changes gradually with composition from ~3.3 for ITO to ~3.0 for $x = 0.28$ in $In_{2-2x}Cd_xSn_xO_3$.[37] Finally, co-doping was shown to yield p_{O_2}-independent TCO properties. Such "self-doped" behavior eliminates the need for a reduction step. Alternatively, such

materials should prove more robust during processing which involves both oxidizing and reducing steps.

Acknowledgements

This work was supported in part by the MRSEC program of the National Science Foundation (DMR-0076097) and in part by the U.S. Department of Energy (FG02-84ER45097) and through the National Renewable Energy Lab under subcontract AAD-9-18668-05. DRK acknowledges the support of an NSF graduate fellowship. The authors are grateful to James D. Jorgensen and Jason P. Hodges for assistance with the neutron diffraction experiments and to John Quintana for help with anomalous X-ray and EXAFS experiments. The work at Argonne National Laboratory was supported by the Department of Energy, Office of Science, under contract W-31-109-ENG-38.

References

1 D. S. Ginley and C. Bright, *MRS Bull.*, 2000, **28**, 15–18.
2 M. Marezio, *Acta. Crystallogr.*, 1966, **20**, 723–728.
3 J. H. W. de Wit, *J. Solid State Chem.*, 1973, **8**, 142–149; J. H. W. de Wit, *J. Solid State Chem.*, 1975, **13**, 192–200; J. H. W. de Wit, *J. Solid State Chem.*, 1977, **20**, 143–148.
4 G. Frank and H. Köstlin, *Appl. Phys. A*, 1982, **27**, 197–206.
5 K. Sasaki, H. P. Siefert and L. J. Gauckler, *J. Electrochem. Soc.*, 1994, **141**, 2759–2768.
6 J.-H. Hwang, D. D. Edwards, D. R. Kammler and T. O. Mason, *Solid State Ionics*, 2000, **129**, 135–144.
7 T. O. Mason, G. B. González, D. R. Kammler, N. Mansourian-Hadavi and B. J. Ingram, *Thin Solid Films*, 2002, **411**, 106–114.
8 O. Warschkow, D. E. Ellis, G. B. González and T. O. Mason, *J. Am. Ceram. Soc.*, submitted.
9 O. Warschkow, D. E. Ellis, G. B. González and T. O. Mason, *J. Am. Ceram. Soc.*, submitted.
10 D. R. Kammler, B. J. Harder, N. W. Hrabe, N. M. McDonald, G. B. González, D. A. Penake and T. O. Mason, *J. Am. Ceram. Soc.*, in press.
11 D. R. Kammler, D. D. Edwards, B. J. Ingram, T. O. Mason, G. B. Palmer, A. Ambrosini and K. R. Poeppelmeier, in *Photovoltaics for the 21st Century*, ed. V. K. Kapur, R. D. McConnell, D. Carlson, G. P. Ceasar and A. Rohatgi, PV 99-11, The Electrochemical Society, Pennington, NJ, 1999, pp. 68–77.
12 R. Y. Korotkov, J. M. Gregie and B. W. Wessels, *Opto-Electron. Rev.*, 2002, **10**, 243–249.
13 H. Reiss, C. S. Fuller and F. J. Morin, *Bell Syst. Tech. J.*, 1956, **35**, 535–636.
14 H. Reiss, C. S. Fuller and A. J. Pietruszkievicz, *J. Chem. Phys.*, 1956, **25**, 650–655.
15 J. A. Van Vechten, J. D. Zook, R. D. Horning and B. Goldenberg, *Jpn. J. Appl. Phys.*, 1992, **31**, 3662–3663.
16 H. Katayama-Yoshida, R. Kato and T. Yamamoto, *J. Cryst. Growth*, 2001, **231**, 428–436.
17 Y. Ohya, T. Ito, M. Kaneko, T. Ban and Y. Takahashi, *J. Ceram. Soc. Jpn.*, 2000, **108**, 803–806.
18 J. L. Bates, C. W. Griffin, D. D. Marchant and J. E. Garnier, *Am. Ceram. Soc. Bull.*, 1986, **65**, 673–678.
19 H. Enoki, J. Echigoya and H. Suto, *J. Mater. Soc.*, 1991, **26**, 4110–4115.
20 D. D. Edwards and T. O. Mason, *J. Am. Ceram. Soc.*, 1998, **81**, 3285–3292.
21 J. D. Jorgensen, J. Faber, J. M. Carpenter, R. K. Crawford, J. R. Haumann, R. L. Hitterman, R. Kleb, G. E. Ostrowski, F. J. Rotella and T. G. Worlton, *J. Appl. Crystallogr.*, 1989, **22**, 321–333.
22 G. Evans and R. F. Pettifer, *J. Appl. Crystallogr.*, 2001, **34**, 82–86.
23 H. Rietveld, *J. Appl. Crystallogr.*, 1969, **2**, 65–71.
24 J. Rodríguez-Carvajal, *Reference Guide for the Computer Program FullProf*, Laboratoire Leon Brillouin, CEA-CNRS, Saclay, France, 1997.
25 T. Ressler, *J. Synchrotron Radiat.*, 1998, **5**, 118–122.
26 F. M. Smits, *Bell Syst. Tech. J.*, 1958, **37**, 711–718.
27 T. Maruyama, Y. Saito, M. Shinohara, Y. Aoyama and W. Komatsu, in *Electro-Ceramics and Solid-State Ionics*, ed. H. L. Tuller and D. M. Smyth, PV 88-3, The Electrochemical Society, Pennington, NJ, 1988, pp. 104–111.
28 G. B. González, J. B. Cohen, J.-H. Hwang, T. O. Mason, J. P. Hodges and J. D. Jorgensen, *J. Appl. Phys.*, 2001, **89**, 2550–2555.
29 Ph. Parent, H. Dexpert, G. Tourillon and J. M. Grimal, *J. Electrochem. Soc.*, 1992, **139**, 276–281; Ph. Parent, H. Dexpert, G. Tourillon and J. M. Grimal, *J. Electrochem. Soc.*, 1992, 282–285.
30 N. Nadaud, N. Lequeux, M. Nanot, J. Jove and T. Roisnel, *J. Solid State Chem.*, 1998, **135**, 140–148.
31 O. N. Myrasov and A. J. Freeman, *Phys. Rev. B.*, 2001, 64, 233 111: 1–3.
32 R. D. Shannon, *Acta Crystallogr., Sect. A*, 1976, **A32**, 751–767.
33 D. S. Maclachlan, M. Blaszkiewicz and R. E. Newnham, *J. Am. Ceram. Soc.*, 1990, **73**, 2187–2203.
34 A. Ambrosini, S. Malo, K. R. Poeppelmeier, M. A. Lane, C. R. Kannewurf and T. O. Mason, *Chem. Mater.*, 2002, **14**, 58–63.
35 G. P. Palmer and K. R. Poeppelmeier, *Chem. Mater.*, 1997, **9**, 3121–3126.
36 R. D. Shannon, J. L. Gillson and R. J. Bouchard, *J. Phys. Chem. Solids*, 1977, **38**, 877–881.
37 D. R. Kammler, T. O. Mason and K. R. Poeppelmeier, *J. Am. Ceram. Soc.*, 2001, **84**, 1004–1009.
38 O. Warschkow and D. E. Ellis, personal communication.
39 D. Ko, K. R. Poeppelmeier, D. R. Kammler, G. B. Gonzalez, T. O. Mason, D. L. Williamson, D. L. Young and T. J. Coutts, *J. Solid State Chem.*, 2002, **163**, 259–266.
40 S. B. Zhang and S.-H. Wei, *Appl. Phys. Lett.*, 2002, **80**, 1376–1378.